

Production and decay of $\Sigma(1660)$ †

S. P. Apsell,* P. Ford,† S. Gourevitch, L. E. Kirsch, and P. E. Schmidt
Department of Physics, Brandeis University, Waltham, Massachusetts 02154

C. Y. Chang, A. R. Stottlemyer,§ and G. B. Yodh
Department of Physics and Astronomy, University of Maryland, College Park, Maryland 20742

S. Glickman,|| M. Goldberg, S. M. Jacobs,¶ B. Meadows,** and G. C. Moneti
Department of Physics, Syracuse University, Syracuse, New York 13210

J. Brenner, J. Schneps, and G. Wolsky
Department of Physics, Tufts University, Medford, Massachusetts 02155
 (Received 8 April 1974)

An investigation has been performed of some properties of $\Sigma(1660)$ produced in the reaction $K^-p \rightarrow \Sigma^+(1660)\pi^-$ at 2.87 GeV/c incident K^- momentum. The decay modes observed for this state include $\Lambda(1405)\pi$ and $\Sigma\pi$. The spin and parity are measured to be $J^P = \frac{3}{2}^-$. The differential cross section of the $\Lambda(1405)\pi$ decay mode is sharply peaked in the forward direction, falling exponentially with a slope of 5.6 ± 0.7 (GeV/c) $^{-2}$, while the slope for the $\Sigma^0\pi^+$ decay mode is 2.1 ± 0.4 (GeV/c) $^{-2}$. The difference in the ratio of backward to total events for the two decay modes also suggests that two $\Sigma(1660)$'s exist.

There have been observations of a $\Sigma(1660)$ resonance in both formation and production experiments.¹ However, there is significant disagreement between the two types of experiments as to the branching ratios for different decay modes. The formation experiments by the CERN-Heidelberg-Saclay collaboration (CHS) measure $\Sigma(1660) \rightarrow \Sigma\pi$ as the dominant mode, whereas $\Sigma(1660) \rightarrow \Lambda(1405)\pi$ is less than 6% of the total rate.² Spin-parity analysis yields a value of $\frac{3}{2}^-$.

The situation for $\Sigma(1660)$ observed in production appears to be reversed. Experiments by Eberhard *et al.*³ and Aguilar-Benitez *et al.*⁴ observe the primary decay to be $\Sigma(1660) \rightarrow \Lambda(1405)\pi$, particularly in the region of small momentum transfer. The authors of Ref. 3 observe little $\Sigma(1660) \rightarrow \Sigma\pi$; however, they note that at large momentum transfers the $\Sigma\pi/\Lambda(1405)\pi$ branching ratio is consistent with that observed in formation experiments. The results of this experiment tend to support these conclusions.

Since the evidence strongly supports the hypothesis that there are two $\Sigma(1660)$ resonances, we choose to define two states: $\Sigma_P(1660)$, with significant coupling to the \bar{K} -nucleon system and with a large decay rate into $\Sigma\pi$, observed predominantly in formation experiments; and $\Sigma_p(1660)$, produced peripherally and having a large decay rate into $\Lambda(1405)\pi$.

In this experiment, we have studied the reaction $K^-p \rightarrow \Sigma^+(1660)\pi^-$ in the following final states:

$$K^-p \rightarrow \Sigma^+ \pi^- \pi^+ \pi^- \left. \vphantom{K^-p} \right\} 16.8 \text{ events}/\mu\text{b}, \quad (1a)$$

$$\Sigma^- \pi^+ \pi^+ \pi^- \left. \vphantom{K^-p} \right\} 16.8 \text{ events}/\mu\text{b}, \quad (1b)$$

$$\Sigma^+ \pi^0 \pi^- \quad 10.2 \text{ events}/\mu\text{b}, \quad (2a)$$

$$\Sigma^0 \pi^+ \pi^- \left. \vphantom{K^-p} \right\} 23.1 \text{ events}/\mu\text{b} \quad (2b)$$

$$\Lambda^0 \pi^+ \pi^- \quad 23.1 \text{ events}/\mu\text{b} \quad (3)$$

$$\Lambda^0 \pi^+ \pi^0 \pi^- \quad 23.1 \text{ events}/\mu\text{b} \quad (4)$$

$$\bar{K}^0 p \pi^- \quad 23.1 \text{ events}/\mu\text{b} \quad (5)$$

from a 10⁶-picture exposure at 2.87 GeV/c in the 31-in. BNL hydrogen bubble chamber. Different samples of the exposure were used for the study of different reactions, and the sensitivity for each is given in reactions (1)–(5).

I. EVENT SELECTION

The events used in this experiment are derived from two distinct topologies observed in the bubble chamber.

Reactions (1) and (2a) are selected by scanning for a kinking track (the Σ^\pm decay) plus one or three additional prongs. Reactions (2b), (3), (4), and (5) are selected by scanning for a "V" plus two charged prongs.

A. Charged Σ events—selection criteria

The kinematic fitting probability distributions for these events deviated significantly from uni-

formity below 2% for the 4-prong events and below 5% for the 2-prong events. Hence, these became the minimum acceptable values for the fit probability. Moreover, there is a low efficiency for detecting charged Σ 's which decay close to the production vertex, or for which the projected decay angle is small. Examination of the scanning detection efficiency showed that a sharp decline in the number of events found occurred when this angle was less than 5° . Finally, a fiducial volume, which permitted an adequate distance for measurement of the momenta of all tracks, was defined.

The final selection criteria for an event to remain in the sample are given below:

1. *4-prong topology.*

- (a) fit probability $\geq 2\%$ (4 constraints),
- (b) kink projected length ≥ 0.3 cm,
- (c) kink projected angle $\geq 5^\circ$.

2. *2-prong topology.*

- (a) fit probability $\geq 5\%$ (1 constraint),
- (b) kink projected length ≥ 0.5 cm,
- (c) kink projected angle $\geq 5^\circ$,
- (d) kink dip angle $\leq 60^\circ$.

Since the desired final state from the latter topology has weakly constrained fits, the kinematic fitting program may obtain several acceptable solutions for each event. Approximately 50% of the events have a unique solution, and an additional 30% have two solutions. The remaining events are rejected because of multiple solutions, and a correction is made for their loss. As a check on the purity of the sample we have examined the missing mass. Since the momentum of the Σ is generally not measurable, because of its short track length, and is calculated only from the decay angle and momentum of the decay track, the missing mass is poorly resolved. For events that fit, however, this shows a peak at about the π^0 mass with a broad flat background, indicating that there is no sizeable contamination of multiple π^0 events.

Each acceptable event was then weighted by the inverse of the probability that the geometric selection criteria were satisfied.

To check for scanning or selection biases, the lifetime and center-of-mass decay angle distribution were calculated from the weighted events. The lifetime distributions show exponential decay with values of the mean lifetime in agreement with those reported by the Particle Data Group.⁵ The decay-angle distributions in the Σ rest frame, which are expected to be isotropic, show a small loss of events at center-of-mass angles corresponding to the cutoff at 5° for the projected decay angle in the laboratory. As a final check we find that the measured ratio of the $\Sigma^+ \rightarrow p\pi^0/\Sigma^+ \rightarrow n\pi^+$ is in agreement with the reported average value.

From an initial measurement of approximately

15 000 events of each topology, the final sample contained 3466 events of reaction (1) and 2137 events of reaction (2a).

The scanning and measuring efficiencies were determined from careful double scanning of a subsample of the data. Physicists examined every event of the single kink topology which failed to fit reactions (1) or (2a) or reaction (1) with an additional π^0 or reaction (2a) without π^0 . The overall efficiency (the product of the scanning, measuring, processing and geometric detection efficiencies) for observing events of reaction (1) is 0.57 ± 0.03 and that for reaction (2a) is 0.43 ± 0.03 .

B. Neutral Σ and Λ events—selection criteria

The difficulty in the selection of events belonging to reactions (2b), (3), and (4) stems from the large number of ambiguities in the kinematic fitting of these events.

An event is considered to have made a successful fit if the probability (χ^2) is greater than 1% for reaction (3) and greater than 5% for reactions (2b) and (4). A count of the ambiguities based on fitting alone is given in Table I. Since it is impossible to completely separate these channels without any losses, we have used a set of criteria which minimizes the contamination and results in a calculable loss of events. First we assume that any event which makes a unique fit to reaction (3) belongs to that channel. The remainder of the events are sorted without recourse to the quality of their kinematic fits.

The events which are ambiguous between $\Lambda^0\pi^+\pi^-$ and $\Sigma^0\pi^+\pi^-$ belong mainly to the former reaction since it is more tightly constrained. In order to study the ambiguity we use the fitted quantities and plot the cosine of the angle between the Λ^0 in the Σ^0 center-of-mass system and the direction

$$\hat{Z} = \frac{(\hat{K}^- \times \hat{\Sigma}^0) \times \hat{\Sigma}^0}{|(\hat{K}^- \times \hat{\Sigma}^0) \times \hat{\Sigma}^0|},$$

where the momenta are in the laboratory frame. If a true Σ^0 event is produced, the Λ^0 is correlated neither with the Σ^0 direction nor with the normal to the production plane. This distribution is shown

TABLE I. Fit ambiguities for events belonging to the two-prong +V topology ($0.70 < \hat{K}^- \cdot \hat{\pi}^- < 1.0$).

	$\Lambda^0\pi^+\pi^-$	$\Sigma^0\pi^+\pi^-$	$\Lambda^0\pi^+\pi^-\pi^0$
$\Lambda^0\pi^+\pi^-$	783	931	11
$\Sigma^0\pi^+\pi^-$		327	263
$\Lambda^0\pi^+\pi^-\pi^0$			3100
3-fold = 85			

for the events which are ambiguous in Fig. 1(a) and for the events which uniquely fit $\Sigma^0\pi^+\pi^-$ in Fig. 1(b). It is expected that the true Σ^0 events will display a uniform distribution as is observed in Fig. 1(b). This uniformity indicates that there is no measurable contamination of the $\Sigma^0\pi^+\pi^-$ events by the $\Lambda^0\pi^+\pi^-$ and that events displaying the kinematic ambiguity can be treated as belonging wholly to the latter reaction.

The events which are ambiguous between $\Sigma^0\pi^+\pi^-$ and $\Lambda^0\pi^+\pi^-$ belong largely to the former reaction. This ambiguity was studied by assuming that the reaction is $\Lambda^0\pi^+\pi^-X$, where X is the missing mass. In the vicinity of zero, the $M^2(X)$ distribution is a Gaussian with a full width of ~ 0.02 GeV $^2/c^2$. Thus, it is impossible to make a complete separation of these two channels. In order to obtain as pure and unbiased a sample of events from reaction (2b) as possible, we have required that an event meet three criteria: (1) a successful $\Sigma^0\pi^+\pi^-$ fit, (2) $1.10 < M^2(\Lambda X) < 1.70$ GeV $^2/c^4$, and (3) $-0.04 < M^2(X) < 0.02$ GeV $^2/c^4$.

The data are displayed in Figs. 2(a), 2(b). The contamination of the sample, as determined by extrapolation of a flat background beyond the Σ^0 and γ peaks, is less than 11%. This procedure results in a loss of those events which fail to make the kinematic fit. Applying criteria (2) and (3) to this sample shown in Figs. 2(c), 2(d), and then fitting the $M^2(X)$ distribution to a Gaussian centered at $X=0$, indicates that 321 events have been lost. However, the effective mass of $\pi^+\pi^-X$ for these events shows that 81 are really η^0 decays, reducing the number of Σ^0 events lost to 240.

Since the $\Lambda^0\pi^+\pi^-$ and $\Lambda^0\pi^+\pi^-\pi^0$ channels show small cross contamination and contain a large number of events relative to the number in the $\Sigma^0\pi^+\pi^-$ channel, they are used without any further selections.

The over-all detection efficiencies, including the probability for charged Λ^0 decay, for reactions (2b), (3), and (4) are 0.23 ± 0.03 , 0.37 ± 0.03 , and 0.36 ± 0.03 , respectively.

Since there is negligible ambiguity between Λ^0 and K^0 decays, events which fit reaction (5) are accepted without further selections.

The flux for this topology in the data was determined⁶ to be 23.1 events/ μ b.

II. PRODUCTION OF $\Sigma^+(1660) \rightarrow \Lambda^0(1405)\pi^+$

The $\Sigma^+\pi^+\pi^+$ effective mass spectrum from reaction (1) shows a strong $\Sigma(1660)$ signal. In order to determine the branching ratio

$$R \equiv \frac{\Sigma_P^+(1660) \rightarrow \Lambda^0(1405)\pi^+}{\Sigma_P^+(1660) \rightarrow (\Sigma\pi\pi)^+}$$

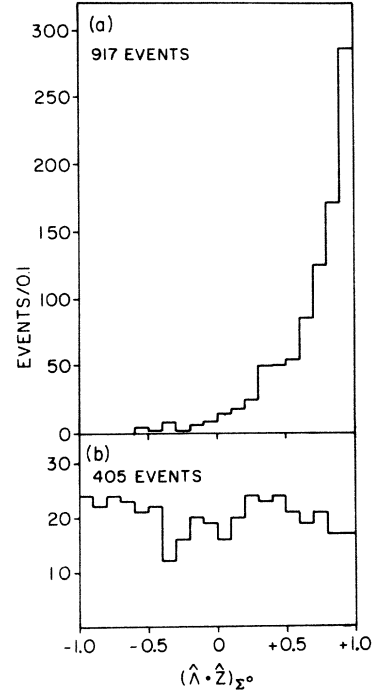


FIG. 1. (a) Angular distribution $\hat{\Lambda}^0 \cdot \hat{Z}$ (see text for definition of \hat{Z}) for events which are ambiguous between $\Lambda^0\pi^+\pi^-$ and $\Sigma^0\pi^+\pi^-$. (b) Same as (a) for events which satisfy $\Sigma^0\pi^+\pi^-$ selection criteria.

we use only the $\Sigma^-\pi^+\pi^-\pi^-$ events for which $1630 < M(\Sigma^-\pi^+\pi^-) < 1690$ MeV $^2/c^2$ since the $\Sigma^+\pi^-\pi^-\pi^-$ final state with two $(\Sigma\pi\pi)^+$ mass combinations is more difficult to analyze. Since peripheral production is the dominant process, we also restrict the production angle to $0.7 < \cos\theta^* < 1.0$, where $\cos\theta^* = \hat{K}^- \cdot \hat{\pi}^-$. The resulting data sample has only a small amount of background in the $\Sigma(1660)$ mass region, and studies of control regions are consistent with this belonging to the $\Lambda^0(1405)\pi^+\pi^-$ channel. A fit to the data gives $R = 1.00 \pm 0.02$, which is consistent with all decays occurring via the $\Lambda^0(1405)\pi$ intermediate state.

The determination of the differential cross section for $\Sigma(1660)$ production is made by first selecting those events for which the $(\Sigma\pi)^0$ mass, shown in Fig. 3, lies near the $\Lambda(1405)$ [$1365 < M(\Sigma\pi)^0 < 1445$ MeV $^2/c^2$] and then treating the final state as $\Lambda^0(1405)\pi^+\pi^-$. This substantially reduces the background, as can be seen in the $\Lambda^0(1405)\pi^+$ mass spectrum shown in Fig. 4.

The treatment of final state $\Sigma^+\pi^-\pi^+\pi^-$ differs slightly from $\Sigma^-\pi^+\pi^+\pi^-$ since in the former case there are two possible $\Sigma^+(1660)$ production angles. In this case each event is treated as if it were two events, each with a weight of 0.5. However, this is a small effect since only 1% of these events

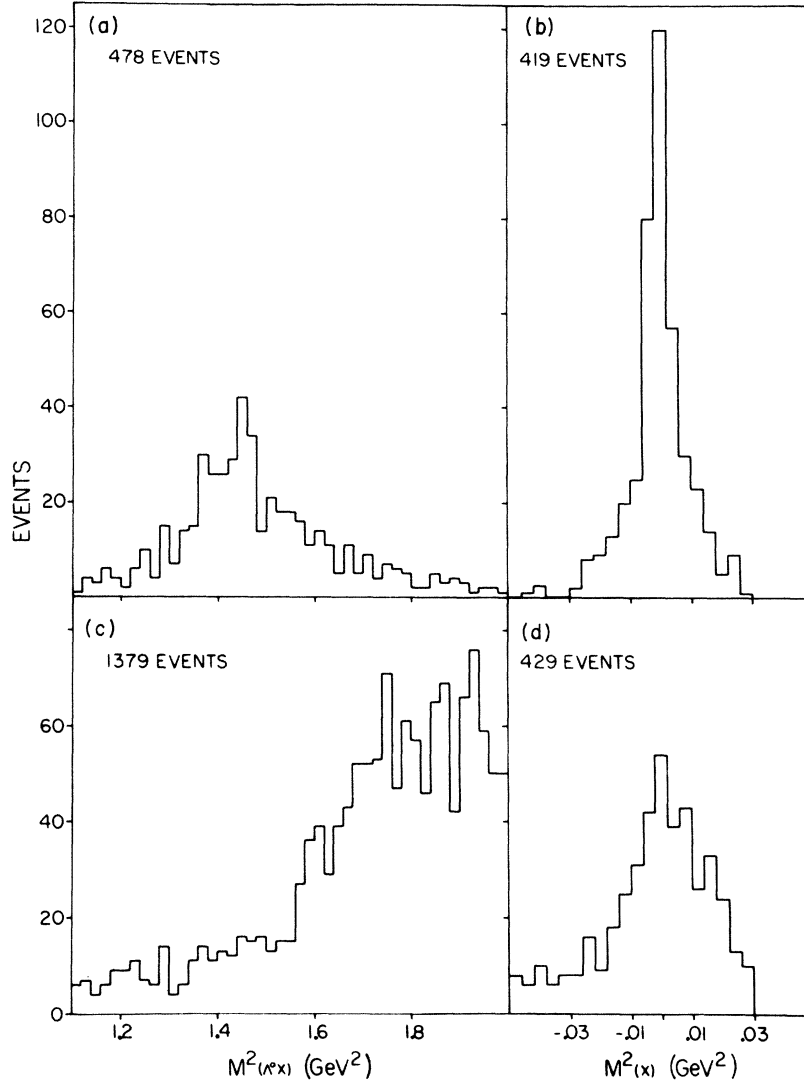


FIG. 2. (a) Effective mass squared $\Lambda^0 X$ from the state $\Lambda^0 \pi^+ \pi^- X$ for events which have an acceptable kinematic fit to the $\Sigma^0 \pi^+ \pi^-$ hypothesis. (b) Missing mass squared X for events in (a) with $1.1 < M^2(\Lambda X) \leq 1.7$. (c) Same as (a) for events which do not have an acceptable $\Sigma^0 \pi^+ \pi^-$ fit. (d) Same as (b) for events which do not have an acceptable $\Sigma^0 \pi^+ \pi^-$ fit.

have two $\Sigma^+ \pi^-$ mass combinations near the $\Lambda^0(1405)$ and at least one production angle in the forward region.

The maximum-likelihood method was used to fit the data in each of four production angular regions to determine the number of $\Sigma_P^+(1660)$ events. The differential cross sections are given in Table II and shown in Fig. 5. The parameters of the $\Sigma(1660)$ determined from a fit to all the events in the angular region $0.7-1.0$ are $M_0 = 1665 \pm 1.0$ MeV/c², $\Gamma = 67 \pm 2.4$ MeV.

The differential cross section for the decay mode $\Sigma^+(1660) \rightarrow \Lambda(1405) \pi^+$ falls rapidly with momentum transfer and can be represented as

$$\frac{d\sigma}{dt}(K^- p \rightarrow \Sigma_P^+(1660) \pi^-) = \frac{d\sigma}{dt} \Big|_{t=0} e^{-b|t|}$$

$\Lambda(1405) \pi^+$

where $b = 5.6 \pm 0.7$ (GeV/c)⁻². This distribution displays a t dependence quite characteristic of two-body processes. For example, in our data

$$\frac{d\sigma}{dt}(K^- p \rightarrow \Sigma^+ \pi^-) = \frac{d\sigma}{dt} \Big|_{t=0} e^{-b'|t|},$$

with $b' = 6.4 \pm 0.3$ (GeV/c)⁻². Such a strong t dependence is typical of channels proceeding by single-meson or Reggeon exchange, which in this

case would be $K^*(890)$ and $K^{**}(1420)$. Direct evidence for vector-meson exchange will be given in the discussion of the parity of the $\Sigma(1660)$.

The above results suggest that this may be a possible mechanism for production of the $\Sigma_P(1660)$. With the dominant coupling $g_{\rho K^* \Sigma_P}$ but $g_{\rho K \Sigma_P} \ll g_{\rho K \Sigma_P'}$, the $\Sigma_P(1660)$ would be difficult to observe in formation experiments. A natural generalization of this idea is that there exist *entire multiplets* of particles which are coupled primarily to the vector or tensor mesons and *can be observed only in production experiments*. A mechanism for this occurs naturally in at least one model within the $SU(6) \times O(3)$ multiplet scheme.⁷ In the $70^- L=1$ multiplet there exist two octets, one of which has a quark spin whose associated amplitude is subject to possible destructive interference in the small-momentum-transfer region we are observing.

III. $\Sigma(1660) \rightarrow \Sigma\pi$

We have examined reactions (2a) and (2b) for other evidence of a state in the 1660 MeV/ c^2 mass region. Again the maximum-likelihood method was used to determine the amount of $\Sigma(1660)$ as a function of production angle. The mass and width were fixed by the $\Sigma_P(1660)$, and no interference with resonances in other channels was assumed. The data are shown in Fig. 6 and the results given in Table II.

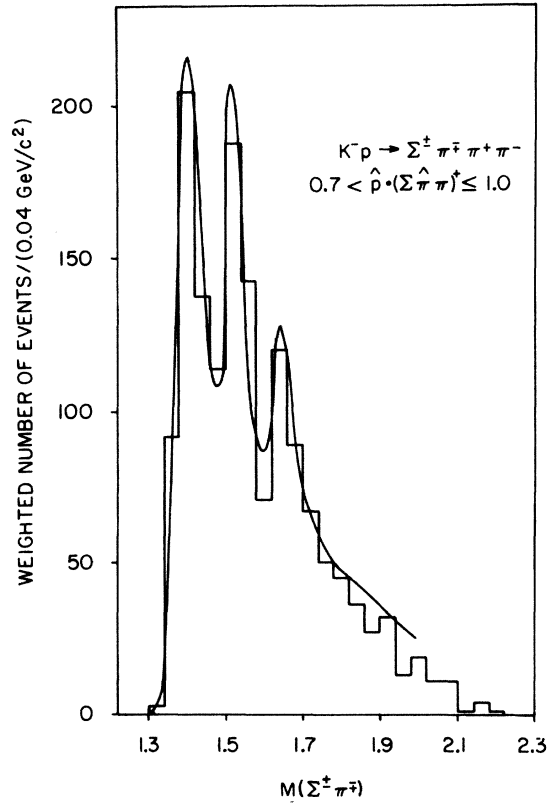


FIG. 3. Effective mass $\Sigma^+ \pi^+$ from the final state $\Sigma^+ \pi^+ \pi^+ \pi^-$.

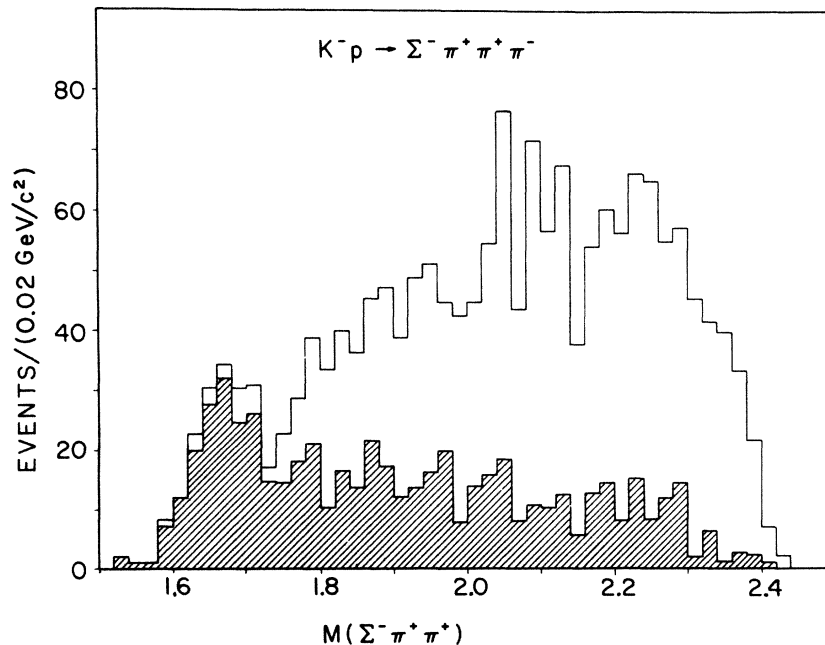


FIG. 4. Effective mass $\Sigma^- \pi^+ \pi^+$ for all events. Shaded region contains the same data with the $\Lambda^0(1405)$ selected.

TABLE II. $\Sigma(1660)$ differential cross section ($\mu\text{b}/\text{sr}$) for the reaction $K^-p \rightarrow \Sigma^+(1660)\pi^-$.

Final state	Production-angle interval $\cos\theta^*$			
	-1.0-0.70	0.70-0.90	0.90-0.95	0.90-1.0
$\Lambda^0(1405)\pi^+$	0.2 ± 0.1	6.5 ± 0.8	23.4 ± 2.4	27.1 ± 2.2
$\Sigma^0\pi^+$	1.6 ± 0.3	7.2 ± 1.0	12.6 ± 2.1	15.9 ± 4.0

The differential cross section for $K^-p \rightarrow \Sigma^+(1660)\pi^-$, $\Sigma^+(1660) \rightarrow \Sigma^0\pi^+$ in the forward production angle region can be represented by an exponential:

$$\frac{d\sigma}{dt}(K^-p \rightarrow \Sigma^+(1660)\pi^-) = \frac{d\sigma}{dt}\Big|_{t=0} e^{-b|t|}$$

\downarrow
 $\Sigma^0\pi^+$

with $b = 2.1 \pm 0.4$ (GeV/c) $^{-2}$.

As a check on the $\Sigma\pi$ final state, we can compare the differential cross sections in reactions (2a) and (2b). While there is no obvious $\Sigma(1660)$ signal in the $\Sigma^+\pi^0$ final state, this could be due to two differences: the higher background resulting from substantial $\Sigma^+\rho^-$ production in the competing channel, and the poor mass resolution of the $\Sigma^+\pi^0\pi^-$ final state. For the purpose of comparison only, we have made a determination of the differential cross section for this process in the production angular region $0.70 < \cos\theta^* < 1.0$, and obtain

$$\frac{d\sigma}{d\Omega}(\Sigma^+(1660) \rightarrow \Sigma^+\pi^0) = 8.6 \pm 2.0 \mu\text{b}/\text{sr},$$

where the error is only statistical. Since this is consistent with the value $9.6 \pm 1.0 \mu\text{b}/\text{sr}$ for the $\Sigma^0\pi^+$ final state, we shall assume that the cross sections measured in the $\Sigma^0\pi^+\pi^-$ channel give the correct production rate.

In the experiment of Eberhard *et al.*,³ it was concluded that there exists a $\Sigma_P(1660)$ different from the $\Sigma_F(1660)$ since the ratio of $\Sigma(1660)$ decaying into $\Sigma^+\pi^+\pi^+$ and $\Sigma^0\pi^+$ varied strongly as a function of the production angle. For the purpose of comparing data from various experiments we define here as a quantitative measure of this variation the angle

$$\chi \equiv \tan^{-1} \left\{ \left[\frac{d\sigma}{d(\cos\theta^*)}(\Lambda(1405)\pi^+) \right] / \left[\frac{d\sigma}{d(\cos\theta^*)}(\Sigma\pi^+) \right] \right\}.$$

Eberhard *et al.* found that this angle changed from $(75.0^{+9.3}_{-9.3})^\circ$ in the production angular region $0.95-1.0$ to $(24.4^{+12.1}_{-8.1})^\circ$ in the region $0.70-0.90$, in comparison to the CHS data, which give a value of less than 15.9° for this angle. This is interpreted as indicating the presence of two resonances.

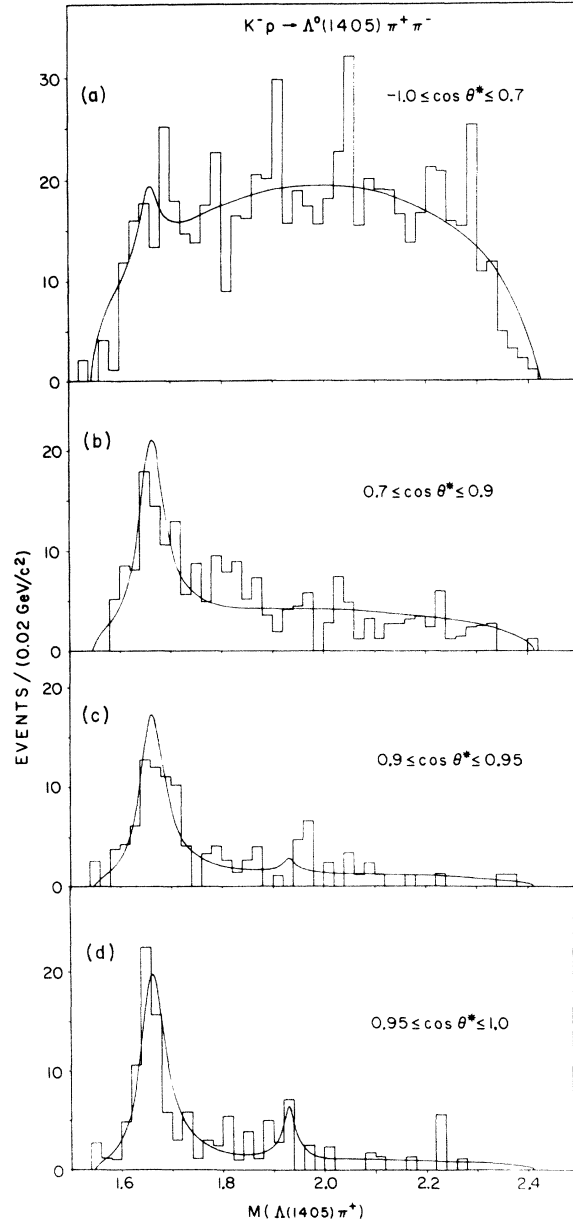


FIG. 5. Effective mass for $\Lambda^0(1405)\pi^+$ for events with production angle $\cos\theta^* = \hat{K}^- \cdot \hat{\pi}^-$ in the range (a) $-1.00 < \cos\theta^* < 0.70$; (b) $0.70 < \cos\theta^* < 0.90$; (c) $0.90 < \cos\theta^* < 0.95$; (d) $0.95 < \cos\theta^* < 1.00$.

Our data for the same angular regions yield the values $\chi = (40.4^{+10.5}_{-8.4})^\circ$ and $(24.3^{+6.2}_{-5.1})^\circ$, which display less variation with production angle.

The other evidence for two $\Sigma(1660)$'s in production experiments is a measurement of the fraction of events in the "backward" angular production region ($-1.0 < \cos\theta^* < 0.70$) obtained for the $\Sigma^+\pi^+\pi^+$ and $\Sigma^0\pi^+$ decay modes. Defining the ratio $\alpha \equiv$ "backward" events/total events, Aguilar-Benitez *et al.*⁴ obtained

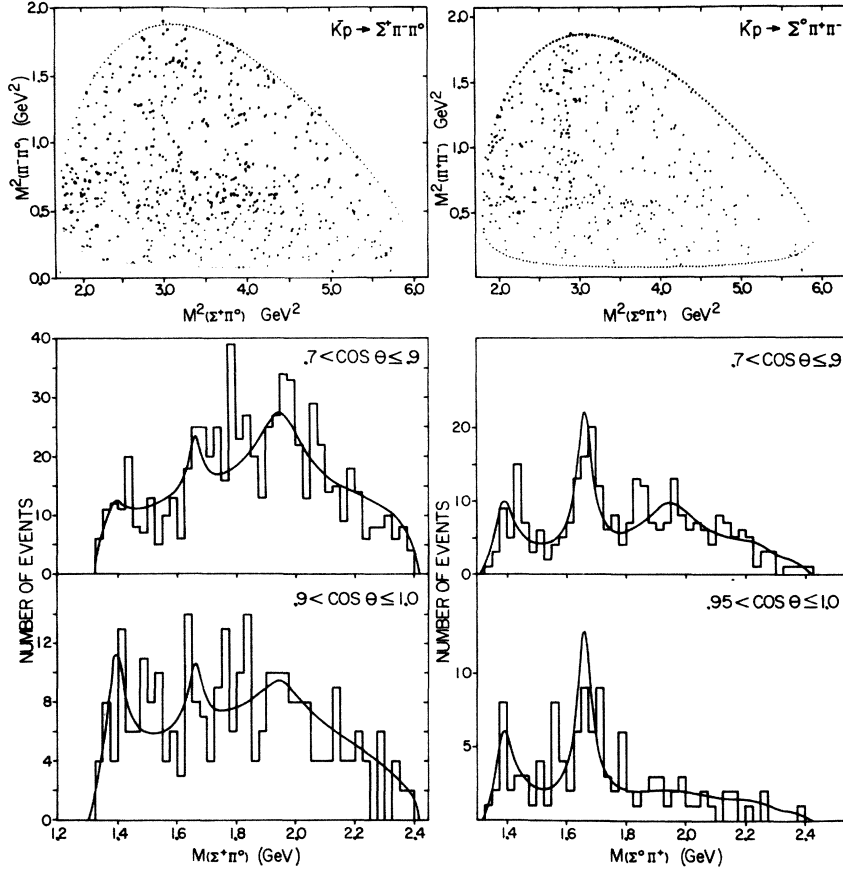


FIG. 6. Dalitz plot and $(\Sigma\pi)^+$ effective mass projection for the final states $\Sigma^+\pi^0\pi^-$ and $\Sigma^0\pi^+\pi^-$ showing the results of the fit for the amount of $\Sigma(1660)$.

$$\alpha(\Sigma\pi\pi) = 0.00 \pm 0.04,$$

$$\alpha(\Sigma^0\pi^+) = 0.42 \pm 0.08.$$

This result is supported by the work of the Nijmegen-Amsterdam collaboration.⁸ We measure

$$\alpha(\Sigma\pi\pi) = 0.18 \pm 0.05,$$

$$\alpha(\Sigma^0\pi^+) = 0.49 \pm 0.11,$$

which provides evidence that this effect persists, although it is less pronounced, at lower energies.

The result can also be expressed in terms of the angle defined above. For this angular region we calculate $\chi = (1.7^{+5.9}_{-4.1})^\circ$, which is well within the limit set by the CHS experiment.

Reactions (3)–(5) were also examined for evidence of other decay modes for $\Sigma(1660)$. These reactions result from different intermediate states, making this extraction of the $\Sigma(1660)$ signal more difficult. In the $\Lambda^0\pi^+\pi^-$ channel, there exists a $\Sigma(1765)$ which overlaps the $\Sigma(1660)$. The results on the differential cross sections are sensitive

to the widths and positions of the resonances and cannot be considered reliable.

In the $\Lambda^0\pi^+\pi^-\pi^0$ channel, there is evidence for a broad peripherally produced enhancement in the $\Lambda^0\pi^+\pi^0$ mass spectrum at about 1660 MeV/ c^2 , which appears to be mainly $\Sigma^+(1385)\pi^0$. This final state also exhibits a number of two- and three-body intermediate states with strong dynamical correlations which may contribute to the bump in the mass spectrum. The width of the peak, and the change in its central value for different production-angle regions indicates that this effect may not be associated with the $\Sigma(1660)$.

Finally, no $\Sigma(1660)$ signal is seen in the $\bar{K}^0p\pi^-$ final state. The data for all these reactions are shown in Fig. 7.

IV. SPIN

If two particles exist which have the same isospin and mass, then it seems highly unlikely that they will have identical spin. Previous evidence⁹ for the $\frac{3}{2}$ spin assignment of $\Sigma_p(1660) \rightarrow \Lambda(1405)\pi$ is

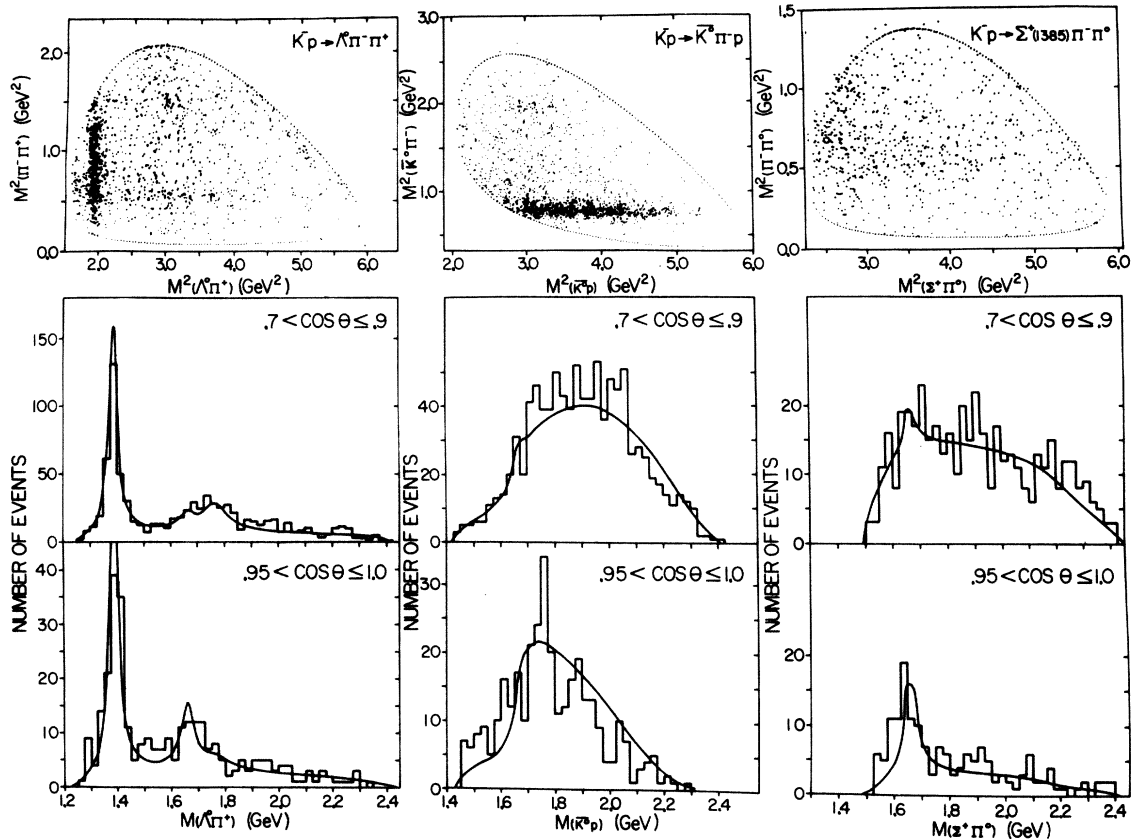
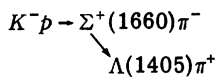


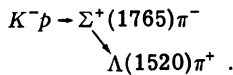
FIG. 7. Dalitz plot and effective mass projections for the strangeness equals -1 baryon, showing the results of a fit for the amount of $\Sigma(1660)$, for the final states: $\Lambda^0 \pi^- \pi^+$, $\bar{K}^0 \pi^- p$, $\Sigma^+(1385) \pi^- \pi^0$.

based in part on the Adair analysis.¹⁰ In Fig. 8(a) we show the experimental Adair distribution for



accompanied by the theoretical distributions for several spin assumptions. From a least-squares fit we find that the probability of $\frac{3}{2}$ spin assignment is 0.17, while that of spin $\frac{5}{2}$ is 0.08, which is a weak indication for the former.

As a check on the validity of the Adair method in the above state, we have also applied it to a similar intermediate state of reaction (1):



The $\Sigma^+(1765)$ is known to have $J^P = \frac{5}{2}^-$ and decay into $\Lambda^0(1520) \pi^+$; the $\Lambda^0(1520)$ has $J^P = \frac{3}{2}^-$. The Adair angular distribution for this reaction is shown in Fig. 8(b) with the theoretical distribution for $J^P = \frac{5}{2}^-$ and p -wave decay. There is a clear disagreement which persists when f -wave decay and f - p interference are included.

The failure of the Adair analysis when applied

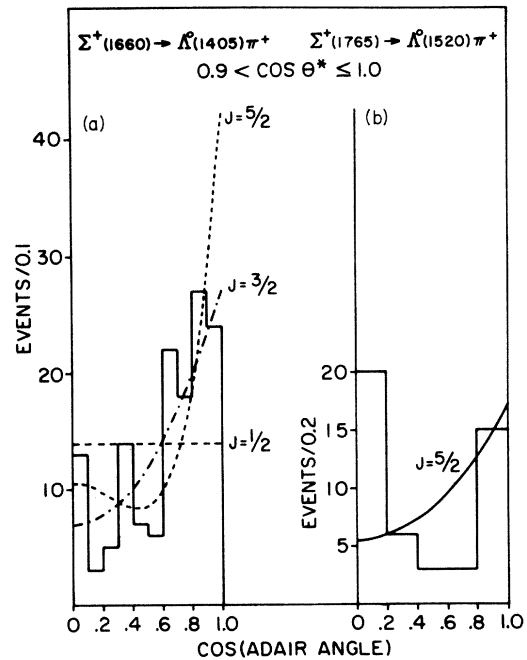


FIG. 8. Adair angular distribution: $\cos(\text{Adair angle}) = \hat{\Lambda}_{\Sigma^* \text{c.m.}} \cdot \hat{\Sigma}_{\text{total c.m.}}^*$

to the $\Sigma(1765)$ may, of course, simply be due to background or interference effects. On the other hand, its apparent success for the $\Sigma_P(1660)$ may be fortuitous; the $\Sigma(1765)$ difficulties are a signal for caution. In fact, a specific example of such a failure is given by Stodolsky and Sakurai¹¹: If vector-meson exchange is dominant, as is likely in this case, and if the vector meson behaves like a massive photon in that the reaction $\bar{K}^* + N \rightarrow \Sigma^* + \Lambda^0 \pi^+$ (at the baryon vertex of the meson-exchange diagram) is dominated by the $M1 - P_{3/2}$ transition, then there will be no events in precisely that region in which the Adair analysis is valid. Bearing in mind such a possibility, we seek to confirm the $\Sigma_P(1660)$ spin by also employing other methods of spin-parity analysis.

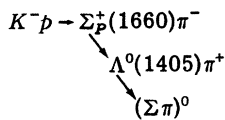
A more general procedure for determining the spin and parity of particles that does not depend on this limitation has been suggested by Byers and Fenster and extended by Button-Shafer.¹² This method was applied to the $\Sigma(1765)$ and the results are shown in Fig. 9. While the angular distributions do not distinguish a $J^P = \frac{5}{2}^-$ from a $\frac{7}{2}^+$ assignment, explicit calculations of the tensor moments do favor the former, giving confidence in this procedure.

The application of the Byers-Fenster method to the $\Sigma_P(1660)$ is much more difficult since the spin of the $\Lambda^0(1405)$ is $\frac{1}{2}$, hence the single angular distribution which distinguishes the spin for the $\Sigma(1765)$ by measuring the relative population of the $\pm \frac{3}{2}$ to the $\pm \frac{1}{2}$ projection is not available for the $\Sigma(1660)$.

In the Byers-Fenster method there are two distributions we can study¹³ to obtain information on the tensor moments describing the production of the $\Sigma_P(1660)$. In both cases, the *highest-L, non-zero tensor moment* gives the *lower limit* on the spin. The first distribution is that of the decay angle of the $\Lambda^0(1405)$ in the $\Sigma_P(1660)$ center-of-mass system:

$$I(\theta) = \sum_{L_{\text{even}}=0}^{2J-1} a_L \cos^{2L}\theta,$$

where the a_L 's are linear combinations of the tensor moments. Another distribution is derived from the decay chain



which ends in the parity-violating $\Sigma - N\pi$ decay. The distribution of the angle χ between the normal to the production plane of the Σ and the nucleon is

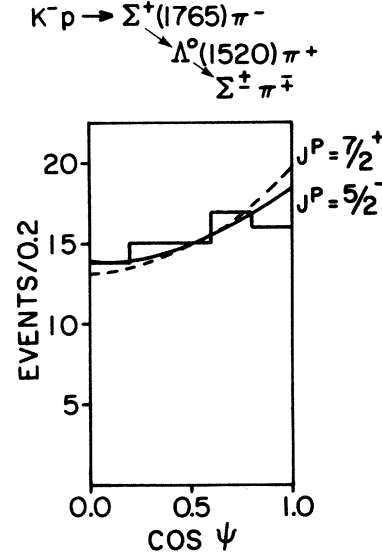


FIG. 9. Angular distribution for Byers-Fenster method of spin-parity analysis. $\cos\psi = \hat{\Lambda}(1520)_{\Sigma(1765)} \cdot \hat{\Sigma}_{\Lambda(1520)}$.

$$I(\theta, \psi, \chi) = 1 + \alpha_{\Sigma} \left[\left(\sum_{L_{\text{odd}}=1}^{2J} a_L \cos^{2L}\theta \right) \cos\psi \right] \cos\chi,$$

where ψ is the decay angle of the Σ in the $\Lambda^0(1405)$ rest system, and α_{Σ} is the Σ decay parameter. Maximum-likelihood fits to these distributions rule out spin $\frac{1}{2}$ but fail to discriminate spin $\frac{3}{2}$ from higher spins in our data. Thus, this method cannot be used to confirm the assignment of $J = \frac{3}{2}$ for the $\Sigma_P(1660)$ from the Adair analysis.

V. $\Sigma(1660)$ PARITY

Previous experiments, using several methods, have given conflicting results for the parity of the $\Sigma_P(1660)$.⁹ As we have noted above, the decay of the $\Sigma_P^+(1660) - \Lambda^0(1405) \pi^+$ precludes the possibility of a determination of the parity using the model-independent Byers-Fenster method.

We can, however, attempt to measure the parity of the $\Sigma_P(1660)$ using the following assumptions:

- The production process proceeds primarily through K^* exchange.
- The conjecture of Stodolsky and Sakurai that vector mesons behave as heavy photons in strong interactions is correct. Thus, photoproduction data imply that the reaction $K^* + N \rightarrow \Sigma^*(1660) + \Lambda^*(1405) \pi$ (at the baryon vertex of the exchange diagram) is dominated by the $M1$ multipole for a $\frac{3}{2}^+$ intermediate state, and by the $E1$ and $L1$ multipoles for the $\frac{3}{2}^-$ state.^{14, 15}

(c) The spin of the $\Sigma_P(1660)$ is $\frac{3}{2}$.

Then the angular distributions for both parities are given by

$$\frac{3}{2}^+ : \frac{d\sigma}{d\Omega} = |M1|^2 [1 + 3(\hat{q} \cdot \hat{n})^2],$$

$$\frac{3}{2}^- : \frac{d\sigma}{d\Omega} = |E1|^2 [1 + 3(\hat{q} \cdot \hat{\epsilon})^2] + 4 |L1|^2 [1 + 3(\hat{q} \cdot \hat{k})^2] - 12 \text{Re}(E1^* L1) (\hat{q} \cdot \hat{\epsilon}) (\hat{q} \cdot \hat{k}),$$

where, for the reaction $\bar{K}p \rightarrow \Sigma^* \pi_1$, $\Sigma^* \rightarrow \Lambda^* \pi_2$, the vectors \hat{q} , \hat{n} , $\hat{\epsilon}$, and \hat{k} are defined using the momenta of the particles in the Σ^* center-of-mass system as follows:

$$\begin{aligned} \hat{q} &= \hat{\pi}_2, \\ \hat{k} &= \hat{K} - \hat{\pi}_1, \\ \hat{n} &= \hat{K} \times \hat{\pi}_1, \\ \hat{\epsilon} &= \hat{n} \times \hat{k}, \end{aligned}$$

and $M1$, $E1$, and $L1$ are the amplitudes of the respective multipoles.

The results are shown in Fig. 10. The probability for spin $\frac{3}{2}$ and odd parity is 0.23, while the probability for even parity¹⁶ is $< 10^{-4}$.

The goodness of fit for odd parity confirms the assumptions made above. The excellent agreement of our data with the $E1, L1 - P_{3/2}$ transition also indicates that the Adair analysis should be valid since this transition does not cause a depletion of events at forward production angles. The same method was applied to the reaction $K^- p \rightarrow \Sigma^0 \pi^+ \pi^-$; however, the results are less reliable because of the higher background in the $\Sigma(1660)$ mass region. The data indicate a slight preference for $J^P = \frac{3}{2}^-$ rather than $\frac{3}{2}^+$, but neither assignment can be excluded.

VI. CONCLUSIONS

A. Concerning the existence of two $\Sigma(1660)$'s

There are three sets of measurements on the $\Sigma^+ \pi^+ \pi^+$ and $\Sigma^0 \pi^+$ decay modes which give rise to the conjecture that two resonances exist at this mass:

- (1) The angle χ , measuring the ratio of differential cross sections for the two decay modes, varies with the production angle and disagrees with the value given by the CHS data in the most forward region.
- (2) The slope β of the exponential representing the differential cross sections in the forward region differs for the two decay modes.
- (3) The ratio α measuring the "backward" to total fraction of events differs for the two decay modes.

The first measurement, which is contained in the work of Eberhard *et al.*,³ is perhaps more difficult since it depends on the ratio of cross sections of different decay modes and thus on their different efficiency corrections. Our data, when

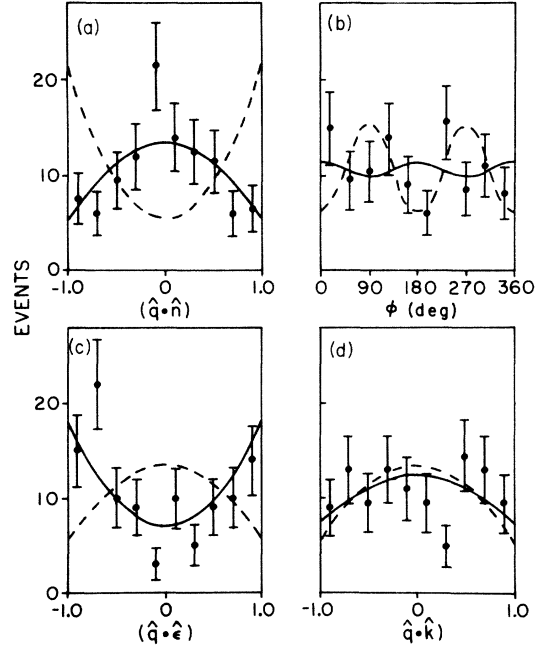


FIG. 10. Angular distributions for Stodolsky-Sakurai method of spin-parity analysis: The unit vectors are described in the text, with $\cos \phi = \hat{n} \cdot (\hat{k} \times \hat{q}) / |\hat{k} \times \hat{q}|$. The dashed (solid) curve is the prediction for $J^P = \frac{3}{2}^+ (\frac{3}{2}^-)$. The χ^2 's for the $(\hat{q} \cdot \hat{k})$, $(\hat{q} \cdot \hat{\epsilon})$, $(\hat{q} \cdot \hat{n})$, and ϕ distributions respectively are: for $J^P = \frac{3}{2}^+$ 11.7, 49.1, 89.6, 11.3; for $J^P = \frac{3}{2}^-$ 7.2, 12.9, 8.0, 8.8.

interpreted in this fashion, display less significant variation in two angular regions but are also not consistent with the CHS results in the most forward region.

The second measurement is independent of normalization but it is not directly comparable to the CHS data. The results of the fit to the differential cross section assuming the exponential form are contained in Table III. Again, the data of Eberhard *et al.*³ show very different slopes for the two decay modes. Our data yield values for the slopes which, although not equal, are not sufficiently divergent to require the acceptance of the two-resonance

TABLE III. Parameterization of differential cross sections in the region $0.70 < \cos \theta^* < 1.0$. $d\sigma/d\mu = d\sigma/d\mu|_0 e^{-\beta\mu}$; $\mu \equiv 1 - \cos \theta^*$.

Decay mode	$\frac{d\sigma}{d\mu} _0$	β	χ^2 (1 deg of freedom)
$(\Sigma\pi\pi)^a$	36.5 ± 2.3	8.7 ± 1.2	2.80
$(\Sigma\pi\pi)^b$	71.5 ± 4.5	11.9 ± 0.9	6.70
$(\Sigma^0\pi^+)^a$	17.9 ± 3.6	4.7 ± 0.7	0.00
$(\Sigma^0\pi^+)^b$	9.6 ± 2.1	0.2 ± 1.3	0.76

^aThis experiment.

^bData of Ref. 3.

hypothesis.

The third measurement yields dramatically different results for the two decay modes in our data as well as in those of Aguilar-Benitez *et al.*⁴ and the Nijmegen collaboration.⁸ This is certainly compelling evidence for the existence of $\Sigma_P(1660)$ and $\Sigma_F(1660)$. In light of this result the second measurement suggests that the $\Sigma_P(1660) \rightarrow \Sigma\pi$ decay mode also exists, with the exponential slope perhaps flattened by the contribution of the $\Sigma_F(1660)$ amplitude. Thus, we conclude that two $\Sigma(1660)$'s exist. Both are observed in production experiments with the state having low momentum transfer exhibiting decay modes into $\Lambda(1405)\pi$ and $\Sigma\pi$.

We cannot obtain clear evidence for the existence of $\Lambda\pi$, $\Lambda\pi\pi$, or $\bar{K}^0 p$ decay modes of this resonance.

B. Concerning the spin and parity of the $\Sigma(1660)$'s

It appears that there exist two Σ states with the same mass and identical spin parity. The $\Sigma_F(1660)$ is known to be a D_{13} state. We have used two model-independent techniques to measure the spin of $\Sigma_P(1660)$, and both weakly favor spin $\frac{3}{2}$. Moreover, assuming spin $\frac{3}{2}$ and the applicability of the Stodolsky-Sakurai model, we have obtained strong evidence that the $\Sigma_P(1660)$ has odd parity.

†Research supported in part by the U. S. Atomic Energy Commission and the National Science Foundation.

*Present address: Eikonix Corporation, Burlington, Massachusetts 01803.

‡Present address: University of Paris, Paris, France.

§Present address: Tufts University, Medford, Massachusetts 02155.

|| Present address: Imperial College, London, England.

¶ Present address: Brandeis University, Waltham, Massachusetts 02154.

**Present address: University of Cincinnati, Cincinnati, Ohio 45221.

¹A recent review of the experimental data is given by P. Eberhard, in *Baryon Resonance-73*, edited by E. Fowler (Purdue Univ. Press, Lafayette, Ind., 1973), pp. 247-252.

²R. Armenteros *et al.*, Nucl. Phys. **B14**, 91 (1969).

³P. Eberhard *et al.*, Phys. Rev. Lett. **22**, 200 (1969).

⁴M. Aguilar-Benitez *et al.*, Phys. Rev. Lett. **25**, 58 (1970).

⁵Particle Data Group, Phys. Lett. **50B**, 1 (1974).

⁶S. Jacobs, Ph.D. thesis, Syracuse University, 1972 (unpublished).

⁷D. Faïman, Nucl. Phys. **B32**, 573 (1971).

⁸Nijmegen-Amsterdam Collaboration (unpublished).

⁹A. Leveque *et al.*, Phys. Lett. **18**, 69 (1965); Y. Y. Lee *et al.*, Phys. Rev. Lett. **17**, 45 (1966); P. Eberhard *et al.*, Phys. Rev. **163**, 1446 (1967).

¹⁰R. K. Adair, Phys. Rev. **100**, 1540 (1955).

¹¹L. Stodolsky and J. Sakurai, Phys. Rev. Lett. **11**, 90 (1960); L. Stodolsky, Phys. Rev. **134**, B1099 (1964).

¹²N. Byers and S. Fenster, Phys. Rev. Lett. **11**, 52 (1963); J. Button-Shafer, Phys. Rev. **139**, B607 (1965).

¹³These distributions are derived by L. Kirsch in Brandeis Internal Memo No. 70-01 (unpublished).

¹⁴Although the Stodolsky-Sakurai model makes predictions for baryon resonance decay into a 0^- meson and a $\frac{1}{2}^+$ baryon, one can use it as it stands for decay into a 0^- meson and a $\frac{1}{2}^-$ baryon [the $\Lambda(1405)$] by invoking the Minami ambiguity.

¹⁵See, for example, R. L. Walker, Phys. Rev. **182**, 1729 (1969).

¹⁶If we relax the constraint of the Stodolsky-Sakurai model that vector-meson exchange is dominated by the magnetic dipole transition for even parity, then the $E2$ and $L2$ multipoles may in principle contribute. In that case, we can also obtain a good fit to the data for even parity.